J. metamorphic Geol., 1994, 12, 811–826

Metamorphic *P–T* paths from calcic pelitic schists from the Strafford Dome, Vermont, USA

T. MENARD[1] AND F. S. SPEAR[2]
[1]Department of Geology and Geophysics, University of Calgary, Calgary, Alberta, T2N 1NH Canada
[2]Department of Earth and Environmental Sciences, Rensselaer Polytechnic Institute, Troy, NY 12180, USA

ABSTRACT Metamorphism of the Gile Mountain Formation and Waits River Formation in the Strafford Dome and Townshend–Brownington Syncline in east-central Vermont records two nappe-style events, D1 and D2, followed by doming. D1 formed a muscovite + biotite ± ilmenite schistosity subparallel to compositional layering, S0, and was followed by heating to garnet grade. The temperature and pressure at the end of D1 are estimated to be *c.* 450° C and 6–8 kbar. D2 variably crenulated and folded S1 during a nearly isothermal pressure increase of 1–2 kbar, calculated from compositions of garnet, which have inclusions trails with progressive crenulation and rotation of the S1 fabric. Similar *P–T* paths are computed for most of the area, suggesting that the later schistosity developed during emplacement of a regional nappe 3–6 km thick. There is a general lack of D3 (dome-stage) microstructures.

Near the Strafford–Willoughby Arch, staurolite and kyanite overgrew S2 in pelites, and plagioclase with increasing X_{An} overgrew S2 in calcic pelites, reflecting post-D2 heating to a maximum of 550–600° C. Metamorphic pressures at the end of D2 are fairly constant on the west side of the dome, indicating minor dome-stage uplift. In contrast, pressures at the thermal peak of metamorphism decrease by more than 4 kbar east of the dome. The observed pattern of isotherms and isobars is mainly the result of post-metamorphic, differential uplift and unroofing.

Finally, a minor, retrograde metamorphism produced the assemblage albite + epidote + K-feldspar + muscovite + chlorite, with grade increasing east toward the Connecticut River.

Key words: Acadian metamorphism; calcic pelites; garnet zoning; New England; *P–T* paths; thermobarometry.

INTRODUCTION

Metamorphic pressure–temperature (*P–T*) paths can be used to interpret the thermal and tectonic evolution of a region (e.g. Selverstone *et al.*, 1984; Selverstone & Spear, 1985), and the variation of metamorphic *P–T* paths across a region reflects spatial variation in the thermal and tectonic history. Examples of detailed studies of metamorphic petrology aimed at understanding the tectonic history of western New Hampshire and eastern Vermont include Spear & Rumble (1986), Kohn *et al.* (1992), Spear *et al.* (1990b), Florence *et al.* (1993), Armstrong (1993) and Vance & Holland (1993). These studies provide basic data for regional, tectonic syntheses (e.g. Spear & Harrison, 1990; Armstrong *et al.*, 1992).

In this context, we present data on the Acadian metamorphic history of the Strafford Dome in east-central Vermont (Fig. 1). The Strafford Dome is an excellent location to study metamorphic *P–T* paths in eastern Vermont because metapelitic schists are exposed across the dome and the rocks were affected only by Acadian deformation and metamorphism. We document the variation in metamorphism and *P–T* paths across the dome and correlate metamorphic episodes with the regional deformational events. We concentrate on metamorphism of calcic pelitic schists because they contain mineral assemblages appropriate for *P–T* path studies, because they are common in the field area and because the phase equilibria are well understood (Menard & Spear, 1993).

The Strafford Dome area was recently the subject of several studies of metamorphic fluid flow (Barnett & Chamberlain, 1991; Ferry, 1992; Stern *et al.*, 1992; Hames & Menard, 1993). The present paper provides additional details of the metamorphic setting for those studies.

METHODS

More than 600 samples were collected in the study area (Fig. 2), 330 thin sections were examined petrographically, concentrating on garnet-bearing calcic pelitic schists, and minerals from 40 samples were analysed with the JEOL 733 electron microprobe at Rensselaer Polytechnic Institute. Detailed petrological descriptions of samples featured in this report are given in the Appendix. Details of analytical techniques and mineral compositions were reported by Menard (1991). Garnet compositional zoning was documented with 3–8 radial traverses of 50–300

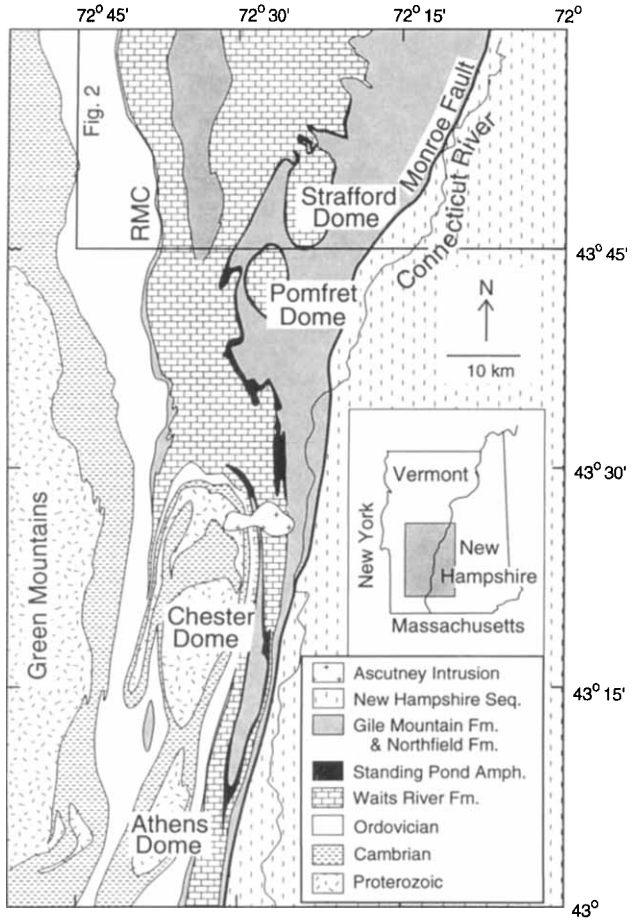

Fig. 1. Geology of south-eastern Vermont (simplified after Doll, 1961). RMC is the contact between the Siluro-Devonian rocks and older rocks to the west. The location of the study area is shown (Fig. 2).

analytical points, with spacing of analyses decreasing to 2 μm near the rim. Plagioclase zoning patterns were determined using backscattered electron imaging, supplemented by spot analyses and line traverses. Compositions of other minerals were determined by multiple spot analyses.

The Gibbs method of differential thermodynamics (Rumble, 1974; Spear *et al.*, 1982; Spear, 1988, 1989) is used here for P–T path calculations (Spear & Selverstone, 1983; Selverstone & Spear, 1985). Most of the necessary thermodynamic data are from Berman (1988), along with data for graphite from Holland & Powell (1990). Thermodynamic data for additional phase components not listed by Berman (1988) were computed using exchange values (Holland, 1989). Mineral compressibilities were computed from the data of Powell & Holland (1988) using the method of Spear *et al.* (1991). A non-ideal equation of state was used for mixed H_2O–CO_2 fluids (Kerrick & Jacobs, 1981) with entropy data for CO_2 from Bottinga & Richet (1981). All solid phases were assumed to be ideal. Gibbs method computations were performed using a FORTRAN computer program on an Apple Macintosh computer (Spear *et al.*, 1991).

The rocks discussed here are calcic pelitic schists that during garnet growth had the assemblage garnet + biotite + chlorite + plagioclase + epidote + quartz + muscovite + graphite + fluid, and minor tourmaline, ilmenite and rutile. This assemblage was used in P–T path calculations by Selverstone & Spear (1985) and Menard & Spear (1993). Compositional variability in the nine-phase assemblage can be modelled in the system SiO_2–Al_2O_3–Fe_2O_3–MgO–FeO–MnO–CaO–Na_2O–K_2O–H_2O–CO_2, which gives a system variance of four. The four monitor variables needed to compute a Gibbs method P–T path were chosen as the garnet and plagioclase compositions, X_{Alm}, X_{Sps}, X_{Grs} and X_{An}, because garnet and plagioclase are compositionally zoned. The sequence of garnet and plagioclase compositions during metamorphism and the correlation of their compositions are critical parts of the petrographic descriptions given in the Appendix.

GEOLOGICAL SETTING

Stratigraphy

The Waits River Formation and Gile Mountain Formation are Silurian to Early Devonian in age, based on plant fossils and U–Pb age dates (Hueber *et al.*, 1990); prior age determinations were contradictory (Doll, 1943; Bothner & Finney, 1986; Spear & Harrison, 1989). Thus, the Waits River Formation and Gile Mountain Formation are younger than the Ordovician Taconian metamorphism that affected older rocks in eastern Vermont (Doll *et al.*, 1961). The Waits River Formation, which comprises micaceous limestones, pelitic schists and the Standing Pond Amphibolite, is older than the Gile Mountain Formation, as shown by stratigraphic tops in graded beds (Fisher & Karabinos, 1980). The Gile Mountain Formation is lithologically similar to the Waits River Formation, but has a greater abundance of quartz + mica schists and amphibolites, and has a lower percentage of limestones (Doll, 1944). Some of the amphibolites are associated with strata-bound volcanogenic copper deposits, including the Elizabeth mine near South Strafford (White & Eric, 1944; Howard, 1969; Annis *et al.*, 1983; Offield & Slack, 1993). The Northfield Formation is a pelitic schist similar to parts of the Gile Mountain Formation that may be older (Doll *et al.*, 1961) or younger than the Waits River Formation (Hatch, 1987). The Waits River, Gile Mountain and Northfield formations in east-central Vermont occupy the Connecticut Valley Trough.

Structural geology

Hatch (1988) interpreted the general structure in the Connecticut Valley Trough as a fault-bounded anticlinorium, in contrast with earlier interpretations (e.g. Doll *et al.*, 1961). On the eastern side of the study area, the Monroe Fault separates Vermont Sequence rocks from New Hampshire Sequence rocks (Fig. 1; Billings, 1956). On the western side of the study area, the contact between Siluro-Devonian rocks in the Connecticut Valley Trough

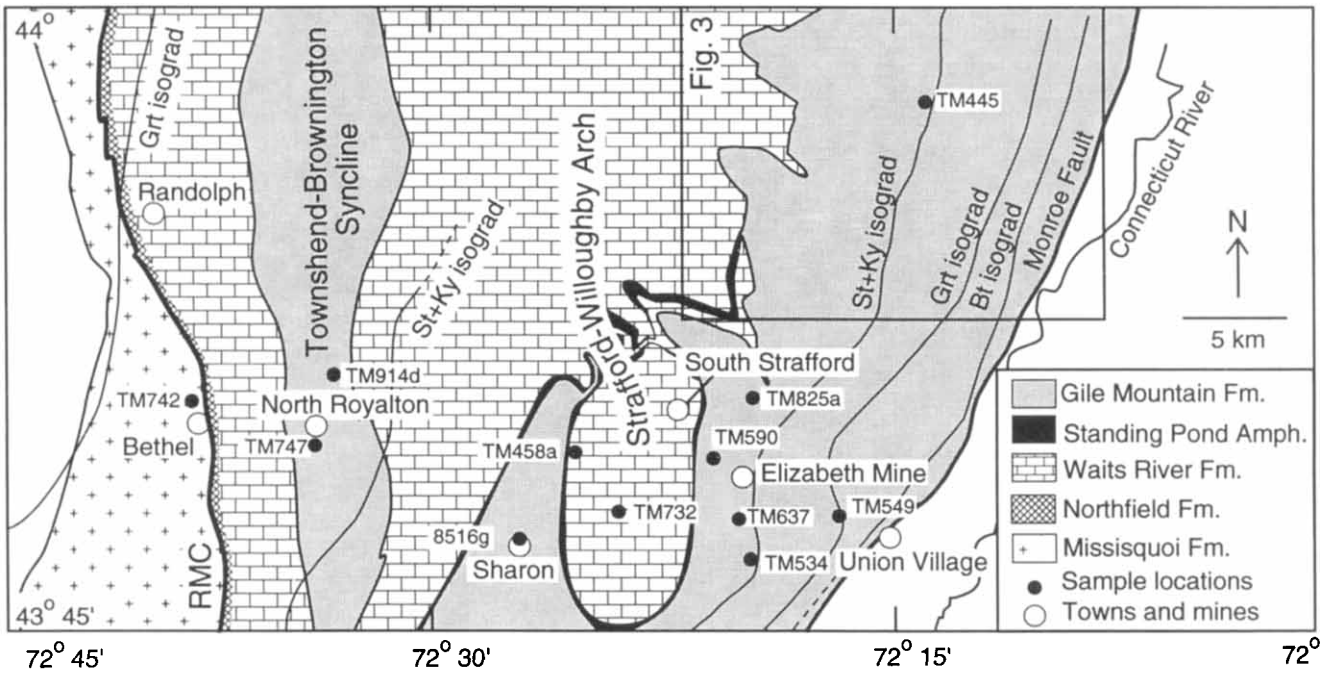

Fig. 2. Geology of the study area after Doll (1943), White & Jahns (1950), Hadley (1950), Ern (1963), Doll *et al.* (1961), Rolph (1982) and Hatch (1987). RMC is the contact between Siluro-Devonian rocks and older rocks to the west. The location of Fig. 3 is shown. Latitude and longitude of samples discussed in text: TM742: 72.64319 W, 43.83980 N; TM747: 72.56588 W, 43.82286 N; TM914D: 72.55817 W, 43.85123 N; TM458A: 72.42775 W, 43.81800 N; TM732: 72.39865 W, 43.79471 N; TM590: 72.33613 W, 43.80578 N; TM549: 72.28266 W, 43.79475 N.

and pre-Silurian rocks to the west is informally known as the Richardson Memorial Contact or RMC (after Richardson, 1919); it is a stratigraphic contact (Doll *et al.*, 1961) or a fault contact (Westerman, 1987; Hatch, 1988). Displacements along the RMC and the Monroe Fault are unknown.

The major structures within the study area (Fig. 2) are the Townshend–Brownington Syncline and the Strafford Dome (Doll, 1944; Doll *et al.*, 1961). The Strafford Dome is the southern portion of the Strafford–Willoughby Arch and is the northernmost of a series of domes in eastern Vermont (Fig. 1), including the Pomfret, Chester, Athens, Rayponda and Guildford domes (Doll *et al.*, 1961).

Minor structures in the study area have been described by Doll (1944), White & Jahns (1950), Hadley (1950), Lyons (1955) and, more recently, by Woodland (1977) near Royalton, and Rolph (1982) and Offield & Slack (1990) near South Strafford. Sedimentary bedding, S0, is locally preserved and is well displayed in graded beds in the Gile Mountain Formation. An early, ductile event, D1, formed a mica schistosity, S1, parallel to S0 and axial to rare F1 folds (White & Jahns, 1950). D1 may have been a nappe-style event, and may be responsible for most of the folding of the Townshend–Brownington Syncline (Woodland, 1977).

S0 and S1 were crenulated and folded by D2, producing the S2 schistosity (White & Jahns, 1950). D2 deformation produced large, recumbent folds that cross the Strafford Dome at South Strafford (White & Jahns, 1950), and may have involved emplacement of a nappe and a possible increase of pressure (Woodland, 1977). The S2 schistosity is horizontal in the core of the Strafford Dome, and elsewhere dips away from the dome (Doll, 1944; White & Eric, 1944; Woodland, 1977), demonstrating that the S2 fabric was domed. The development of the S2 fabric is stronger in the core of the Strafford Dome than on the flanks (White & Jahns, 1950), possibly as a result of exposure of deeper structural levels in the core of the dome.

Metamorphism

Metamorphic phase petrology of calcic pelitic schists from the study area was described by Menard & Spear (1993). Most of the garnet growth in the calcic pelites occurred in the assemblage garnet + biotite + chlorite + plagioclase + epidote + quartz + muscovite + graphite + fluid. Along *P–T* paths of heating, garnet in this assemblage grew with a fairly constant and high X_{Grs} while plagioclase grew with increasing X_{An}. Increasing pressure was recorded by decreasing X_{Grs} and X_{An} during plagioclase consumption. If chlorite was removed from the assemblage first, garnet growth stopped but plagioclase growth continued with increasing X_{An} along paths of heating or decreasing pressure. On the other hand, if epidote was removed first, the assemblage became a simple pelite: along paths of heating, garnet continued to grow with sharply decreasing X_{Grs}, while plagioclase was consumed. After both epidote and chlorite were removed from the assemblage, minor amounts of plagioclase replaced garnet.

Isograds in metapelites show that peak metamorphic grade increased towards the Strafford Dome (Fig. 2; Ern, 1963; Hadley, 1950; Lyons, 1955; Thompson, in Doll *et al.*, 1961; this study). Sillimanite was reported near South Strafford, Vermont, by G. K. Jacobs (in Doll, 1944) in a rock from Whitcomb Hill with the assemblage sillimanite + kyanite + garnet + biotite + K–feldspar + quartz + graphite + opaques, but sillimanite was not found in the present study. At the highest metamorphic grade found, rocks contain kyanite + staurolite + garnet + biotite + muscovite.

Isograds in micaceous limestones in the Waits River Formation in eastern Vermont also show a general increase of metamorphic grade towards the Strafford–Willoughby Arch (Ferry, 1988, 1992). Increasing metamorphic grade is associated with increasing amounts of fluid infiltration required for metamorphic reactions in the micaceous limestones (Ferry, 1992). A maximum in the calculated amount of metamorphic fluid that reacted with rocks is centred along the Strafford–Willoughby Arch and runs through the town of Sharon (Fig. 2). Barnett & Chamberlain (1991) suggested that fluids near South Strafford flowed from the Gile Mountain Formation into the Waits River limestones during metamorphism, based on a systematic change of oxygen and carbon isotope ratios in quartz and calcite from micaceous limestones near South Strafford. Their data do not require fluid flow over large distances. On the other hand, isotopic analyses of minerals from the Waits River Formation collected over a larger area in eastern Vermont support Ferry's (1992) interpretation of regional-scale metamorphic fluid migration (Stern *et al.*, 1992). Hames & Menard (1993) concluded that fluid infiltration and Ca-metasomatism in calcic pelitic schists at Sharon, Vermont, occurred later than prograde garnet growth, based on garnet compositional zoning.

Spear & Harrison (1989) reported a $^{40}Ar/^{39}Ar$ cooling age of 370 ± 15 Ma for hornblende that has S2 orientations in a sample from the Standing Pond Amphibolite on the west side of the Strafford Dome. This date suggests that metamorphism accompanying D2 deformation was Acadian in age. Similar results were obtained by Laird *et al.* (1991) in south-eastern Vermont.

STAGES OF METAMORPHISM

Four stages of metamorphism are separated here on the basis of their relations to microfabrics. The earliest recorded metamorphism, M1, produced minerals aligned in the S1 schistosity that were later crenulated during M2. In the western and central portions of the field area, S1 is a muscovite + biotite + ilmenite schistosity. The widespread occurrence of biotite-grade metamorphism during M1 suggests uniform temperatures during M1 across much of the study area. In contrast, M1 decreases to chlorite grade east of the Strafford Dome (Fig. 3).

Minerals that cross-cut S1 and are aligned in the S2 fabric include biotite, muscovite, some plagioclase and tourmaline. In the western and central portion of the study area, garnet has rotated S1 inclusion trails and pressure shadows in S2, suggesting that across much of the area garnet grew during M2. In contrast, M2 decreases to biotite grade east of the Strafford Dome (Fig. 2), likely the result of subsequent differential uplift.

Peak M3 metamorphic minerals kyanite, staurolite, and portions of garnet, plagioclase and biotite overgrew S1 and S2, as shown by the lack of deflection of the fabric around the minerals and the continuity of the fabric with inclusion trails in the minerals. Dome-stage deformation did not produce a strong microfabric and, consequently, the relation between it and the peak metamorphism is poorly constrained. Peak metamorphism, M3, post-dates M1 and M2, and decreases in grade away from the dome both to the east and the west (Fig. 3), in contrast with M1 and M2 in which grade decreases only to the east.

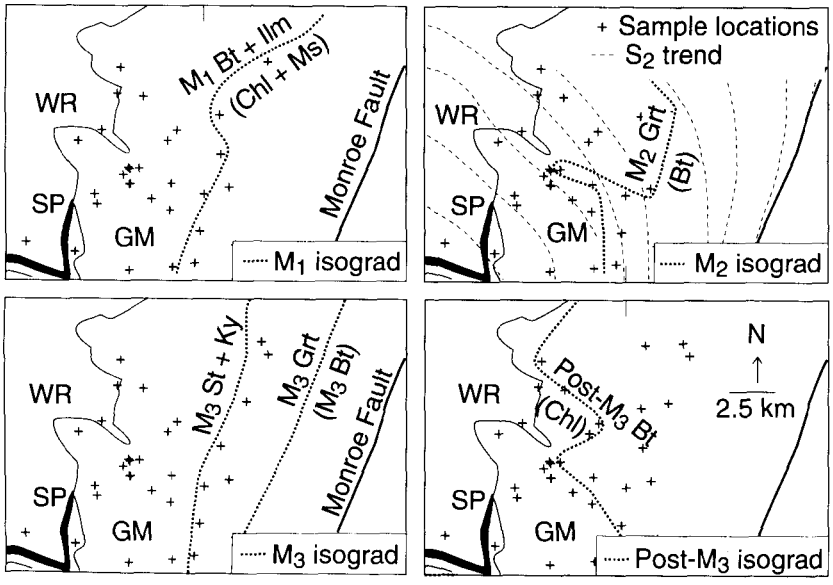

Fig. 3. Metamorphic isograds in the north-east quarter of the Strafford 15′ Quadrangle and the north-west quarter of the Mt Cube 15′ Quadrangle. Metamorphic grade of M1, M2 and M3 increases towards the dome (to the west), while the grade of post-M3 metamorphism increases towards the Monroe Fault. Trend of S2 foliation is from White & Eric (1944) and Hadley (1950). WR, Waits River Formation; SP, Standing Pond Amphibolite; GM, Gile Mountain Formation.

Post-D3 metamorphism produced a widespread, retrograde assemblage of chlorite ± biotite ± calcite + K-feldspar ± sericite, which partially replaced and pseudomorphed M1, M2 and M3 minerals. In the eastern portion of the study area, post-M3 metamorphism increases to biotite grade away from the dome, in contrast with the earlier metamorphic stages (Fig. 3). The timing of this retrogression is uncertain, possibly syn-D4 or syn-D5.

P–T PATHS

Possible errors in *P–T* path computation

Thermobarometric boxes shown in the figures outline intersections of thermometers and barometers for multiple analyses of the minerals. Thus, the boxes represent error associated with real compositional heterogeneity, analytical uncertainty and uncertainty in correlating mineral compositions. Total geological uncertainty, including errors associated with calibrations of the thermometers and barometers, may be on the order of 50° C and a few kilobars (Hodges & McKenna, 1987; Kohn & Spear, 1991). Nevertheless, relative *P–T* errors among samples using a single calibration of a thermometer or barometer will be less than the total geological uncertainty. Metamorphic pressures calculated for samples from the same area (e.g. samples TM914D and TM747) indicate that the magnitude of relative geological uncertainty among samples may be 0.5–1 kbar in this study.

The types, sources and magnitudes of error in *P–T* paths have been discussed previously (e.g. Spear & Rumble, 1986; Spear *et al.*, 1990a,b; Menard, 1991; Kohn, 1993). Errors can accrue from incorrect interpretation of the mineral assemblage or mineral compositional zoning, or from the use of inappropriate thermodynamic data. The shapes of computed Gibbs method *P–T* paths are not strongly dependent on variations in starting values of pressure, temperature, mineral compositions and mineral modes. Instead, because the computations use the differential forms of the thermodynamic equations, the shapes are mainly dependent on the changes used for the monitor variables. Thus, the proper correlation of monitor variables (usually chosen as mineral compositions) is critically important. The sensitivity of computed paths to error in correlation of garnet and plagioclase compositions for the calcic pelite assemblage used here is shown in Table 3. At constant garnet composition, for example, an increase of X_{An} by 0.01 will give $\Delta T = 0.29°$ C, and $\Delta P = -40$ bar, equivalent to the uncertainty in a *P–T* path resulting from propagating an error of $0.01\,X_{An}$ in the correlation of plagioclase compositions with garnet compositions. In a similar manner, propagation of a 0.01 mole fraction error in the garnet compositions results in an error in ΔT and ΔP of approximately 5–6° C and 190–270 bar.

Summary of *P–T* paths

The seven samples described in the Appendix are each representative of compositional, petrographical and microstructural features in a given area. Figure 2 shows the locations of these samples and five other samples in the study area for which *P–T* paths have been described elsewhere (Menard, 1991; Menard & Spear, 1993). Calculated metamorphic *P–T* paths are shown in Figs 4–6.

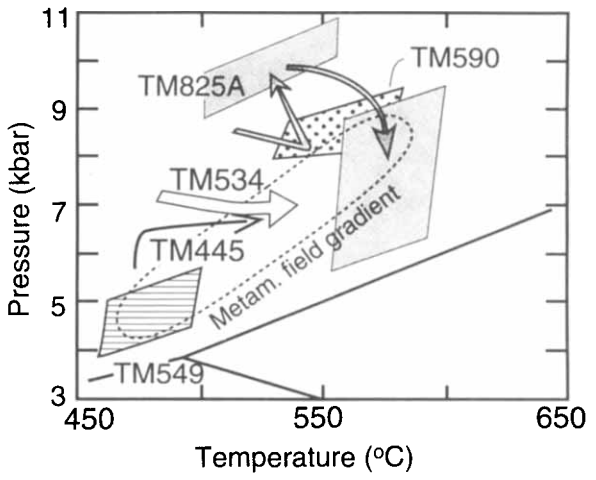

Fig. 4. *P–T* conditions for five samples from the east flank of the Strafford Dome: TM549 at the garnet isograd (ruled box), TM445 (black arrow) and TM534 (white arrow) at staurolite grade, TM825A (shaded arrow) and TM590 (dotted box) at kyanite grade. The final heating in each sample occurred later than the D2 deformation. The differences in pressures at maximum recorded temperature (dashed ellipse) suggest that deeper structurel levels (with higher pressures) are exposed near the core of the dome as the result of post-metamorphic differential uplift. *P–T* boxes for TM825A (shaded) are shown for garnet near-rim and peak metamorphism (Menard & Spear, 1993). The lower temperature portion of the *P–T* path (bent shaded arrow) was calculated from garnet compositional zoning and plagioclase inclusions. The higher temperature part of the path (curved shaded arrow) was based on petrological analysis of late plagioclase and thermobarometry (Menard & Spear, 1993).

The correlation between a given segment of mineral compositional zoning and a specified deformational event is difficult to prove. Factors that contribute to the difficulty include possible variation of styles or intensities of deformational fabrics across an area, and ambiguity in the evidence that a porphyroblast grew prior to, during, or later than a given fabric. As a consequence, we have not tried to prove our interpretations for each rock. Instead, we note the similarity of fabrics across the area (i.e. an earlier schistosity and a later crenulation) and the similarity of mineral compositional zoning patterns that have at least a superficial relation with the two fabrics. Consequently, we correlate the two fabrics across the area with only two events, consistent with Doll (1944) and White & Jahns (1950), and correlate similar patterns in the mineral compositional zoning as having been produced in the same event. Although more complex interpretations can be proposed, we find no evidence to require a more complex interpretation.

The inferred metamorphic conditions during D1 deformation were 400–450° C and 7 kbar in the Strafford

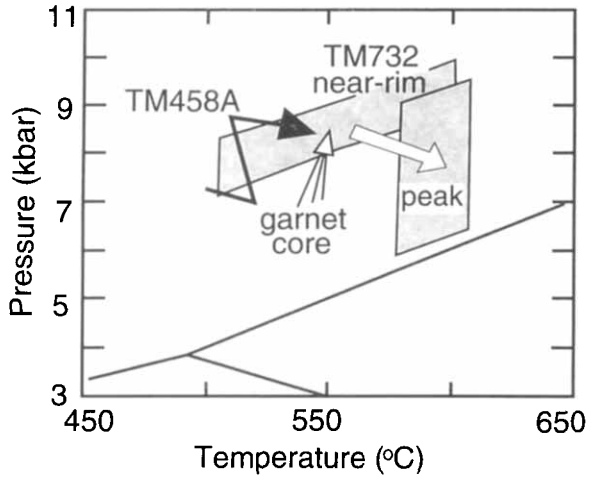

Fig. 5. P–T paths for the Strafford Dome. Thermobarometry for sample TM732 from the core of the dome shows calculated conditions for the garnet near-rim and peak metamorphism (shaded boxes). Three Gibbs method P–T paths for garnet growth (three-legged arrow) were computed with different starting X_{CO_2} (Table 1). The P–T path for late plagioclase growth (white arrow) is inferred from thermobarometry and phase equilibria. The black arrow shows the Gibbs method P–T path for sample TM458A (Table 2) from the west flank of the Strafford Dome. The increase of pressure in both paths correlates with D2.

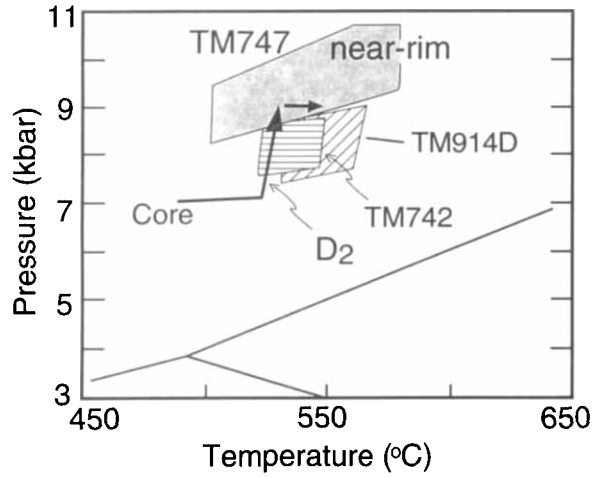

Fig. 6. Thermobarometry and P–T path for samples from the western portion of the study area. The shaded box shows conditions for the garnet near-rim in sample TM747 in the Townshend–Brownington Syncline. The black arrow shows the Gibbs method P–T path for garnet growth (Table 2) with an increase of pressure that roughly coincides with the development of the S2 fabric. Matrix staurolite overgrows the S2 fabric, which suggests a late episode of heating with an indeterminable change of pressure (small black arrow). P–T conditions for sample TM914D in the Townshend–Brownington Syncline (diagonal rule). P–T conditions for the post-D2 garnet rim in sample TM742 (horizontal rule) from Ordovician rocks west of the RMC overlap with those for sample TM914D, suggesting that there was not substantial differential uplift between these two rocks later than D2.

Table 1. Gibbs method models for TM732.

Grt + Bt + Chl + Pl + Ep + Qtz + Ms + Gr + fluid
SiO_2–Al_2O_3–Fe_2O_3–MgO–FeO–MnO–CaO–Na_2O–K_2O–H_2O–CO_2
muscovite $K_{0.85}Na_{0.15}Mg_{0.05}Fe_{0.1}Al_{2.7}Si_{3.15}O_{10}(OH)_2$
biotite $K_{0.86}Na_{0.04}(Mg, Fe, Mn)_{2.5}Al_{1.7}Si_{2.7}O_{10}(OH)_2$
chlorite $(Mg, Fe, Mn)_{4.5}Al_3Si_{2.5}O_{10}(OH)_8$

	Start near-rim	Model 1* Core	Model 2* Core	Model 3* Core
Monitor variables				
X_{Alm}	0.52	0.55	0.55	0.55
X_{Sps}	0.07	0.12	0.12	0.12
X_{Grs}	0.30	0.23	0.23	0.23
X_{An}	0.50	0.65	0.65	0.65
Dependent variables				
T (°C)	550†	537	543	547
P (bar)	8500†	6945	6931	6991
X_{CO_2}	0.50	0.57		
X_{CO_2}	0.10		0.17	
X_{CO_2}	0.01			0.02
X_{Prp}	0.11	0.10	0.10	0.10
X_{Phl}	0.67	0.64	0.64	0.63
X_{Ann}	0.33	0.35	0.36	0.36
X_{Mn-Bt}	<0.01	<0.01	<0.01	<0.01
X_{Mg-Chl}	0.70‡	0.67	0.66	0.66
X_{Fe-Chl}	0.30‡	0.33	0.33	0.33
X_{Mn-Chl}	<0.01§	<0.01	<0.01	<0.01
X_{Czo}	0.50	0.37	0.36	0.36

*The initial fluid composition is not known, so three models were run starting with $X_{CO_2} = 0.5$, 0.10 and 0.01. † Estimated from thermobarometry (Fig. 5). ‡ Estimated using chlorite-garnet thermometry (Dickenson & Hewitt, 1986). § Estimating from chlorite analyses from other rocks (Menard, 1991).

Table 2. Values used in computation of P–T paths.
Sample TM458A

	4 (near rim)	3 (start)	2	1 (core)
Independent variables				
X_{Alm}	0.66	0.64	0.64	0.60
X_{Sps}	0.02	0.03	0.03	0.10
X_{Grs}	0.22	0.26	0.26	0.24
X_{An}	0.32	0.18	0.43	0.25
Dependent variables				
T (°C)	546	510	520	500
P (bar)	8428	8725	7000	7281

Two segments of the path were run starting at point 3. Point labels refer to Fig. 11(b).

Sample TM747

	3 (start)	2	1 (core)
Independent variables			
X_{Alm}	0.67	0.71	0.63
X_{Sps}	<0.01	0.02	0.11
X_{Grs}	0.23	0.19	0.22
X_{An}	0.21	0.32	0.19
Dependent variables			
T (°C)	530	523	489
P (Bar)	9000	7197	7121

Point labels refer to Fig. 12(c).

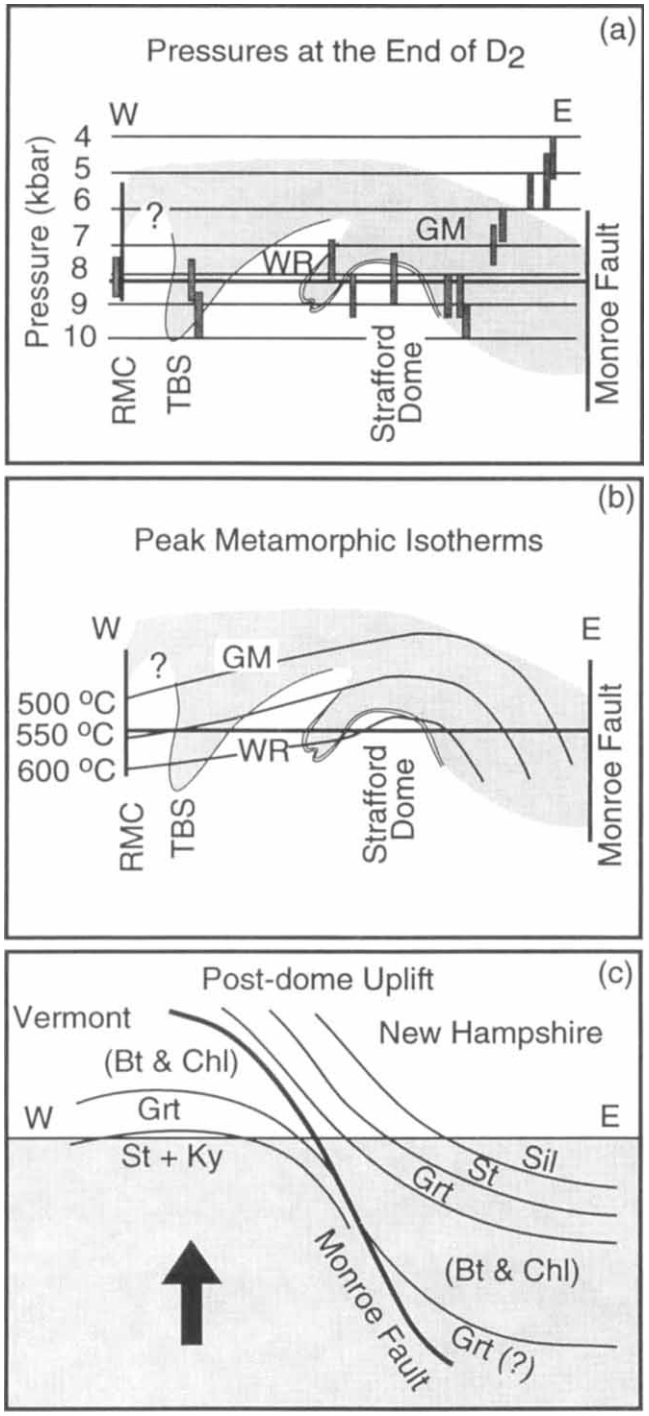

Fig. 7. Sketches of east–west cross-sections. (a) Pressures for post-D2 time (samples described in Appendix, and unpubl. data) superimposed on a cross-section of the major structures. The D3 doming event caused only limited differential uplift, as shown by the similarity of pressures from the RMC to the Strafford Dome. WR, Waits River Formation; GM, Gile Mountain Formation (shaded); RMC, Richardson Memorial Contact; TBS, Townshend–Brownington Syncline. (b) The present distribution of peak metamorphic isotherms superimposed on a cross-section. (c) Interpretative cross-section from eastern Vermont to western New Hampshire showing the post-metamorphic uplift and the present distribution of metamorphic isograds (modified from Spear, 1992). The sketch is not to scale but represents a length across strike of about 75 km. In eastern Vermont, block uplift and denudation exposed rocks in a normal metamorphic sequence with grade decreasing upward, whereas isograds in New Hampshire were inverted (increasing grade upward) by Acadian thrusting. Denudation of Vermont occurred shortly after the Acadian metamorphism, as recorded in hornblende cooling ages (350–380 Ma; Harrison *et al.*, 1989), whereas denudation of New Hampshire took longer (hornblende cooling ages range from 280 to 250 Ma; Harrison *et al.*, 1989). Biotite isograds have been omitted for clarity.

Table 3. Partial derivatives* for garnet growth model for TM732.

	Monitor variables			
	∂X_{Alm}	∂X_{Sps}	∂X_{Grs}	∂X_{An}
Dependent				
∂T (°C)	−515	−575	−563	29
∂P (bar)	−24434	−27076	−18997	<4040
∂X_{Ann}	1.91	0.14	1.43	0.04
∂X_{Mn-Bt}	0.00	0.03	0.00	0.00
∂X_{Fe-Chl}	1.95	0.15	1.49	0.04
∂X_{Mn-Chl}	0.01	0.05	0.01	<0.01
∂X_{CO_2}	−0.88	−0.86	−1.29	−0.14
∂X_{CZO}	−1.18	−1.31	1.32	0.47

*Partial derivatives were computed at starting conditions listed in Table 1 with $X_{CO_2} = 0.01$. Data are shown in form (∂Monitor/∂Dependent) with other monitors constant. Compositions are reported in mole fractions so that a change in X_{Alm} of +0.01, for example, corresponds to a change in T and P of −5° C and −244 bar, respectively.

Dome (e.g. sample TM732) and the Townshend–Brownington Syncline (e.g. sample TM747). D1 deformation was followed by heating.

From Bethel to the Elizabeth Mine, rocks reached garnet grade before D2 deformation started or early during D2 deformation. The second deformational event, D2, produced recumbent F2 folds (Woodland, 1977; Rolph, 1982) during a 1–2 kbar increase of pressure (e.g. samples TM747, TM458A, TM732 & TM825A) and was followed by heating. These paths are similar to models of crustal thickening during thrust faulting or nappe-style deformation (England & Richardson, 1977; England & Thompson, 1984). The similarity of P–T paths during D2 across much of the area (Figs 4–6) suggests that the base of the D2 nappe or thrust fault was at a higher structural level than is exposed at the present erosion surface. This interpretation contrasts with Rosenfeld's (1968) interpretation of the Chester and Athens domes, where the D2 nappe was centred in the Waits River Formation.

D3 domed the S2 fabric (Woodland, 1977) but produced no major fabric. D3 doming produced only minor differential uplift across strike, as indicated by similarity of pressures and temperatures at the end of D2 deformation pressures from the RMC to the Strafford–Willoughby Arch (Fig. 7a). Similar small magnitudes of doming were reported by Armstrong (1993) for the Athens Dome.

Peak metamorphic M3 isograds and temperatures in the

study area are domed (Fig. 7b), with rocks of higher metamorphic grade exposed along the axis of the Strafford–Willoughby Arch than on the flanks. Peak metamorphism, M3, reached temperatures of approximately 540° C in Bethel near the RMC (sample TM742 and unpubl. data), approximately 600° C in the core of the dome (e.g. sample TM732; Fig. 7b), and <400° C near the Monroe Fault. Samples in the Strafford Dome may record a decrease of pressure during heating to peak M3 conditions (e.g. samples TM825A and TM732; Figs 4 & 5).

The variation of peak M3 temperatures from west to east (Fig. 7b) contrasts with the fairly constant M2 temperatures and pressures (Fig. 7a); this contrast is best shown on the western side of the Dome where subsequent differential uplift was minor. The M3 isograds/isotherms do not follow the M2 thermal and baric surfaces. Consequently, the observed distribution of peak temperatures was not produced by differential uplift of an M2–M3 thermal surface. Rather, the thermal structure was different during M2 than during M3. Possible interpretations of the thermal structure include the following.

1 A heat source may have been centred under the dome during M3. Intrusions occur in the core of the Strafford Dome and in the axis of the Strafford–Willoughby Arch: the Brocklebank granite in the northern half of the Strafford Quadrangle, the Knox Mountain pluton east of East Barre and the Willoughby pluton near the Canadian border (Doll, 1944; Doll *et al.*, 1961; Ferry, 1992). If these plutons reflect a buried heat source, then the metamorphic arch may also reflect this heat source.

2 The amount of thermal relaxation and heating following D2 burial may have varied across the area. If post-D3 unroofing proceeded from west to east, the rocks along the Strafford Dome would have remained buried for a few million years longer than the rocks to the west, which could produce the observed difference of 60° C in peak temperature.

3 The thermal properties of the crust may have varied across the area. If the Strafford Dome is cored by Precambrian gneisses with high thermal conductivities, for example, it would have had higher metamorphic temperatures than surrounding rocks.

The broad pattern of increasing peak temperature towards the Strafford–Willoughby Arch at constant pressure was also described by Ferry (1992) for the Waits River Formation in the present study area and areas to the north. The variation in peak metamorphic grade roughly coincides with the variation in the calculated amount of metamorphic fluid flow in mica limestones. Thus, Ferry's (1992) proposed giant, metamorphic hydrothermal system reflects processes near the peak of metamorphism (post–D2) and none of the earlier events. Similarly, the Ca-metasomatism described by Hames & Menard (1993) in calcic pelites from the study area also occurred after the D2 deformation and near the thermal peak of metamorphism.

The thermal peak of metamorphism in eastern Vermont was followed by rapid cooling to 250° C by 310 Ma, presumably due to rapid unroofing (Harrison *et al.*, 1989). Block uplift of the area from Bethel to the Elizabeth Mine is suggested by the calculated metamorphic pressures. On the other hand, the eastern side of the Strafford Dome has a metamorphic field gradient of 3–4 kbar and 100° C (Figs 4 & 7a) over what is now a 4-km cross-strike horizontal distance, indicating significant differential uplift between the Strafford–Willoughby Arch and the Monroe Line.

REGIONAL CORRELATIONS

The Acadian deformational and metamorphic history of the Waits River and Gile Mountain formations in the vicinity of the Strafford Dome is similar to that described for the Chester and Athens domes to the south (Rosenfeld, 1968; Ratcliffe *et al.*, 1992; Armstrong, 1993), although the southern domes also experienced Taconic deformation. Metamorphic P–T paths in the Strafford Dome area are consistent with the interpretation in the Chester Dome of nappes followed by doming (Rosenfeld, 1968). In contrast, we have found no evidence to support the proposal of Bell & Johnson (1989) that the Waits River Formation in eastern Vermont experienced repeated horizontal and vertical compressional events. Our results are also similar to those of Vance & Holland (1993), who calculated a dome-stage P–T path from the Gassetts schist in which pressure decreased from approximately 9.7 to 7.2 kbar during heating to the peak temperature. Vance & Holland noted that because of the mineral assemblage in the rock, and in particular the absence of plagioclase, the pressures in the path have considerable uncertainty; they reported uncertainty in geobarometry of 2.1 kbar, which may serve as an estimate of the uncertainty in the their model P–T path, as well.

The results obtained in this study compare with recent studies of the metamorphism of the adjacent part of western New Hampshire (Spear *et al.*, 1990b; Kohn *et al.*, 1992; Florence *et al.*, 1993; Spear, 1992). Stratigraphy, structures and metamorphic petrology in western New Hampshire demonstrate that metamorphic isograds are inverted, with the highest metamorphic grades in the highest structural levels (Thompson *et al.*, 1968; Spear, 1992). Maximum pressures across western New Hampshire are consistently 4–5 kbar, despite an increase in peak temperature from approximately 450° C in the chlorite zone to over 700° C in the sillimanite zone. In contrast, maximum pressures in Vermont increase dramatically from the Monroe Fault to the Strafford Dome and are nearly constant west of the dome (Fig. 7a) at significantly higher pressures than in New Hampshire. Nevertheless, in both the New Hampshire and Vermont sequences, metamorphic grade decreases to chlorite zone at the Monroe Fault.

Figure 7(c) shows a hypothetical cross-section across eastern Vermont and western New Hampshire, illustrating post-metamorphic differential uplift between the two states and the resulting effects on metamorphic isograds. Spear & Harrison (1990) and Spear (1992) suggested that the entire New Hampshire sequence was emplaced onto Vermont

during Acadian metamorphism, and subsequently was removed along one or more low-angle normal faults in the vicinity of the Monroe line (Fig. 7c). Their interpretation is consistent with our data. We propose that our D2 event reflects the emplacement of the Bronson Hill terrane onto eastern Vermont; the large size of the proposed overthrust is consistent with the scale of collisional tectonic belts.

CONCLUSIONS

Metamorphic P–T paths computed for rocks from the Strafford Dome area generally show heating following the development of S1, followed by an increase of pressure of 1–2 kbar associated with the development of S2, followed by more heating. As expected, garnet growth in some rocks records only portions of the full path. The number and styles of deformations and metamorphisms are similar across most of the study area, which suggests that the tectonic histories were also similar. The P–T paths and thermobarometry suggest that dome-stage deformation produced only a few kilometres of differential uplift. After peak metamorphism, the west side of the study area was uplifted as a block during cooling, with only minor differential uplift of the dome itself, while the east side of the study area (from the Elizabeth Mine to the Monroe Fault) underwent strong differential uplift.

ACKNOWLEDGEMENTS

This paper was part of a doctoral dissertation submitted to Rensselaer Polytechnic Institute (Menard, 1991). Discussions with T. Offield have helped to clarify the structural interpretations. This paper has benefited from reviews by F. P. Florence, T. R. Armstrong, H. W. Day and G. W. Fisher. This research was funded by National Science Foundation grants to F. S. Spear (EAR 87-08609 and EAR 89-16417).

REFERENCES

Annis, M. P., Slack, J. F. & Rolph, A. L., 1983. Stratabound massive sulphide deposits of the Elizabeth Mine, Orange County, Vermont. In: *IGCP-CCSS Symposium Field Trip Guidebook to Stratabound Sulphide Deposits, Bathurst Area, N. B., Canada, and West-Central New England, U.S.A.* (ed. Sangster, D. F.), *Geological Survey of Canada Miscellaneous Report*, **36**, 41–51.

Armstrong, T. R., 1993. Structural and metamorphic constraints on the development of domes in southern Vermont. *Unpubl. PhD Thesis, Virginia Polytechnic Institute & State University.*

Armstrong, T. R., Tracy, R. J. & Hames, W. E., 1992. Contrasting styles of Taconian, eastern Acadian and western Acadian metamorphism, central and western New England. *Journal of Metamorphic Geology*, **10**, 415–426.

Barnett, D. E. & Chamberlain, C. P., 1991. Relative scales of thermal- and fluid-infiltration-driven metamorphism in fold nappes, New England, U.S.A. *American Mineralogist*, **76**, 713–727.

Bell, T. H. & Johnson, S. E., 1989. Porphyroblast inclusion trails: the key to orogenesis. *Journal of Metamorphic Geology*, **7**, 279–310.

Berman, R. G., 1988. Internally-consistent thermodynamic data for minerals in the system Na_2O–K_2O–CaO–MgO–FeO–Fe_2O_3–Al_2O_3–SiO_2–TiO_2–H_2O–CO_2. *Journal of Petrology*, **29**, 445–522.

Billings, M. P., 1956. *The Geology of New Hampshire, part II: Bedrock Geology.* New Hampshire State Planning and Development Commission.

Bothner, W. A. & Finney, S. C., 1986. Ordovician graptolites in central Vermont: Richardson revived. *Geological Society of America Abstracts with Programs*, **18**, 548.

Bottinga, Y. & Richet, P., 1981. High pressure and temperature equation of state and calculation of the thermodynamic properties of gaseous carbon dioxide. *American Journal of Science*, **281**, 615–660.

Dickenson, M. P. & Hewitt, D., 1986. A garnet–chlorite geothermometer. *Geological Society of America Abstracts with Programs*, **18**, 584.

Doll, C. G., 1943. A Paleozoic revision in Vermont. *American Journal of Science*, **241**, 57–63.

Doll, C. G., 1944. A preliminary report on the geology of the Strafford Quadrangle, Vermont. *Vermont Geological Survey, 24th Report of the State Geologist*, 14–28.

Doll, C. G., Cady, W. M. & Thompson, J. B., 1961. Centennial geologic map of Vermont. *Vermont Geological Survey, scale* 1:250,000.

England, P. C. & Richardson, S. W., 1977. The influence of erosion upon the mineral facies of rocks from different metamorphic envrionments. *Journal of the Geological Society of London*, **134**, 201–213.

England, P. C. & Thompson, A. B., 1984. Pressure–temperature–time paths of regional metamorphism I. Heat transfer during the evolution of regions of thickened continental crust. *Journal of Petrology*, **25**, 894–928.

Ern, E. H., 1963. Bedrock geology of the Randolph Quadrangle, Vermont. *Vermont Geological Survey Bulletin*, **21**.

Ferry, J. M., 1988. Infiltration-driven metamorphism in northern New England, USA. *Journal of Petrology*, **29**, 1121–1159.

Ferry, J. M., 1992. Regional metamorphism of the Waits River Formation, eastern Vermont: delineation of a new type of giant hydrothermal system. *Journal of Petrology*, **33**, 45–94.

Fisher, G. W. & Karabinos, P., 1980. Stratigraphic sequence of the Gile Mountain and Waits River Formations near Royalton, Vermont. *Geological Society of America Bulletin*, **91**, 282–286.

Florence, F. P., Spear, F. S & Kohn, M. J., 1993. P–T paths from northwestern New Hampshire: Metamorphic evidence for stacking in a thrust/nappe complex. *American Journal of Science*, **293**, 939–979.

Hadley, J. B., 1950. Geology of the Bradford–Thetford area, Orange County, Vermont. *Vermont Geological Survey Bulletin*, **1**.

Hames, W. E. & Menard T., 1993. Fluid-assisted modification of garnet composition along rims, cracks, and mineral inclusion boundaries in samples of amphibolite facies schists. *American Mineralogist*, **78**, 338–344.

Harrison, T. M, Spear, F. S. & Heizler, M. T., 1989. Geochronologic studies in central New England II: Post-Acadian hinged and differential uplift. *Geology*, **17**, 185–189.

Hatch, N. L., 1987. Lithofacies, stratigraphy, and structure in the rocks of the Connecticut Valley Trough, eastern Vermont. In: *Guidebook for Field Trips in Vermont*, Vol. 2 (ed. Westerman, D. S.), pp. 192–212. New England Intercollegiate Geological Conference.

Hatch, N. L., 1988. New evidence for faulting along the "Monroe Line", Eastern Vermont and westernmost New Hampshire. *American Journal of Science*, **288**, 1–18.

Hodges, K. V. & Crowley, P. D., 1985. Error estimation and empirical geothermobarometry for pelitic systems. *American Mineralogist*, **71**, 702–709.

Hodges, K. V. & McKenna, L. W., 1987. Realistic propagation of uncertainties in geological thermobarometry. *American Mineralogist*, **72**, 671–680.

Hodges, K. V. & Spear, F. S., 1982. Geothermometry, geobarometry and the Al_2SiO_5 triple point at Mt. Mossilauke, New Hampshire. *American Mineralogist*, **67**, 1118–1134.

Hoisch, T. D., 1990. Empirical calibration of six independent geobarometers for the mineral assemblage quartz + muscovite + biotite + plagioclase + garnet. *Contributions to Mineralogy and Petrology*, **104,** 225–234.

Holland, T. J. B., 1989. Dependence of entropy on volume for silicate and oxide minerals: a review and predictive model. *American Mineralogist*, **74,** 5–13.

Holland, T. J. B. & Powell, R., 1990. An enlarged and updated internally consistent thermodynamic dataset with uncertainties and MgO–MnO–FeO–Fe_2O_3–Al_2O_3–TiO_2–SiO_2–C–H_2–O_2. *Journal of Metamorphic Geology*, **8,** 89–124.

Howard, P. F., 1969. The geology of the Elizabeth Mine, Vermont. *Vermont Geological Survey Economic Geology*, **5.**

Hueber, F. M., Brothner, W. A., Hatch, N. L., Finney, S. C. & Aleinikoff, J. N., 1990. Devonian plants from southern Quebec and northern New Hampshire and the age of the Connecticut Valley Trough. *American Journal of Science*, **290,** 360–395.

Kerrick, D. M. & Jacobs, G. K., 1981. A modified Redlich-Kwong equation for H_2O, CO_2, and H_2O–CO_2 mixtures at elevated pressures and temperatures. *American Journal of Science*, **281,** 735–767.

Kohn, M. J., 1993. Uncertaintities in differential thermodynamic (Gibbs' method) P–T paths. *Contributions to Mineralogy and Petrology*, **113,** 24–39.

Kohn, M. J., Orange, D. L., Spear, F. S., Rumble, D. & Harrison, T. M., 1992. Pressure, temperature, and structural evolution of west-central New Hampshire: Hot thrusts over cold basement. *Journal of Petrology*, **33,** 521–556.

Kohn, M. J. & Spear, F. S., 1991. Error propagation for barometers: 2. Application to rocks. *American Mineralogist*, **76,** 138–147.

Laird, J., Kunk, M. J., Boxwell, M. A. & Bothner, W. A., 1991. Acadian metamorphism about the Taconic Line, southeastern Vermont. *Geological Society of America Abstracts with Programs*, **23,** 55.

Lyons, J. B., 1955. Geology of the Hanover Quadrangle, New Hampshire–Vermont. *Bulletin of the Geological Society of America*, **66,** 106–146.

Menard, T., 1991. Metamorphism of calcic pelitic schists, Strafford Dome, Vermont. *Unpubl. PhD Thesis, Rensselaer Polytechnic Institute.*

Menard, T. & Spear, F. S., 1993. Metamorphism of calcic pelitic schists, Strafford Dome, Vermont: Compositional zoning and reaction history. *Journal of Petrology*, **34,** 977–1005.

Offield, T. W. & Slack, J. F., 1990. Polyphase folding and thrust faulting in the Vermont Copper Belt. *Geological Society of America Abstracts with Programs*, **22,** 61.

Offield, T. W. & Slack, J. F., 1993. Structures and origin of the Ely copper deposit, east-central Vermont. *United States Geological Survey Bulletin*, **2038,** 59–68.

Powell, R. & Holland, T. J. B., 1988. An internally consistent thermodynamic dataset with uncertainties and correlations: 3. Applications to geobarometry, worked examples and a computer program. *Journal of Metamorphic Geology*, **6,** 173–204.

Ratcliffe, N., Armstrong, T. & Tracy, R. J., 1992. Relations between tectonic-cover and basement, and metamorphic conditions of formation of the Sadawga, Rayponda and Athens Domes of southern Vermont. In: *Guidebook for Field Trips in the Connecticut Valley Region of Massachusetts and Adjacent States*, Vol. 2 (eds Robinson, P. & Brady, J. B.), pp. 257–290. New England Intercollegiate Geological Conference.

Richardson, C. H., 1919. The Ordovician terranes of eastern Vermont. *Vermont State Geologist Report*, **11,** 45–51.

Rolph, A. L., 1982. Structure and stratigraphy around the Elizabeth mine, Vermont. *Unpubl. MS Thesis, University of Cincinnati.*

Rosenfeld, J. L., 1968. Garnet rotation due to the major Paleozoic deformtions in southeast Vermont. In: *Studies of Appalachian Geology: Northern and Maritime* (eds Zen, E.-A., White, W. S., Hadley, J. B. & Thompson, J. B.), pp. 185–202. Interscience Publishers, New York.

Rumble, D., 1974. Gibbs phase rule and its application to geochemistry. *Journal of the Washington Academy of Science*, **64,** 199–208.

Selverstone, J. & Spear, F. S., 1985. Metamorphic P–T paths from pelitic schists and greenstones from the south-west Tauern Window, eastern Alps. *Journal of Metamorphic Geology*, **3,** 439–465.

Selverstone, J., Spear, F. S., Franz, G. & Morteani, G., 1984. High pressure metamorphism in the SW Tauern window, Australia: P–T paths from hornblende–kyanite–staurolite schists. *Journal of Petrology*, **25,** 501–531.

Spear, F. S., 1988. The Gibbs method and Duhem's theorem: the quantitative relationships among P, T, chemical potential, phase composition, and reaction progress in igneous and metamorphic systems. *Contributions to Mineralogy and Petrology*, **99,** 249–256.

Spear, F. S., 1989. Petrologic determination of metamorphic pressure–temperature–time paths. In: *Metamorphic Pressure–Temperature–Time Paths. Short Course in Geology* (eds Spear, F. S. & Peacock, S. M.), pp. 1–55. American Geophysical Union, Washington, DC.

Spear, F. S., 1992. Inverted metamorphism, P–T paths and cooling history of west-central New Hampshire: Implications for the tectonic evolution of central New England. In: *Guidebook for Field Trips in the Connecticut Valley Region of Massachusetts and Adjacent States*, Vol. 2 (eds Robinson, P. & Brady, J. B.), pp. 446–466. New England Intercollegiate Geological Conference.

Spear, F. S., Ferry, J. M. & Rumble, D., 1982. Analytic formulation of phase equilibria: the Gibbs' method. In: *Characterization of Metamorphism Through Mineral Equilibria. Reviews in Mineralogy*, Vol. 10 (ed. Ferry, J. M.), pp. 105–152. Mineralogical Society of America.

Spear, F. S. & Harrison, T. M., 1989. Geochronologic studies in central New England I. Evidence for pre-Acadian metamorphism in eastern Vermont. *Geology*, **17,** 181–184.

Spear, F. S. & Harrison, T. M., 1990. Post Acadian uplift history of central New England from detailed petrologic and $^{40}Ar/^{39}Ar$ studies. *Geological Society of America Abstracts with Programs*, **22,** 71–72.

Spear, F. S., Kohn, M. J., Florence, F. & Menard, T., 1990a. A model for garnet and plagioclase growth in pelitic schist: implications for thermobarometry and P–T path determinations. *Journal of Metamorphic Geology*, **8,** 683–696.

Spear, F. S., Hickmott, D. D. & Selverstone, J., 1990b. Metamorphic consequences of thrust emplacement, Fall Mountain, New Hampshire. *Geological Society of America Bulletin*, **102,** 1344–1360.

Spear, F. S., Peacock, S. M., Kohn, M. J., Florence, F. P. & Menard, T., 1991. Computer programs for petrologic P–T–t path calculations. *American Mineralogist*, **76,** 2009–2012.

Spear, F. S. & Rumble, D., 1986. Pressure, temperature, and structural evolution of the Orfordville Belt, east-central New Hampshire. *Journal of Petrology*, **27,** 1071–1093.

Spear, F. S. & Selverstone, J., 1983. Quantitative P–T paths from zoned minerals: theory and tectonic applications. *Contributions to Mineralogy and Petrology*, **83,** 348–357.

Stern, L. A., Chamberlain, C. P., Barnett, D. E. & Ferry, J. M., 1992. Stable isotope evidence for regional-scale fluid migration in a Barrovian metamorphic terrane, Vermont, USA. *Contributions to Mineralogy and Petrology*, **112,** 475–489.

Thompson, J. B., Robinson, P., Clifford, T. N. & Trask, N. J., 1968. Nappes and gneiss domes in west-central New England. In: *Studies of Appalachian Geology, Northern and Maritime* (eds Zen, E.-A., White, W. S., Hadley, J. B. & Thompson, J. B.), pp. 203–218. John Wiley, New York.

Vance, D. & Holland, T., 1993. A detailed isotopic and petrological study of a single garnet from the Gassetts schist, Vermont. *Contributions to Mineralogy and Petrology*, **114,** 101–118.

Westerman, D. S., 1987. Structures in the Dog River Fault Zone between Noethfield and Montpelier, Vermont. In: *Guidebook*

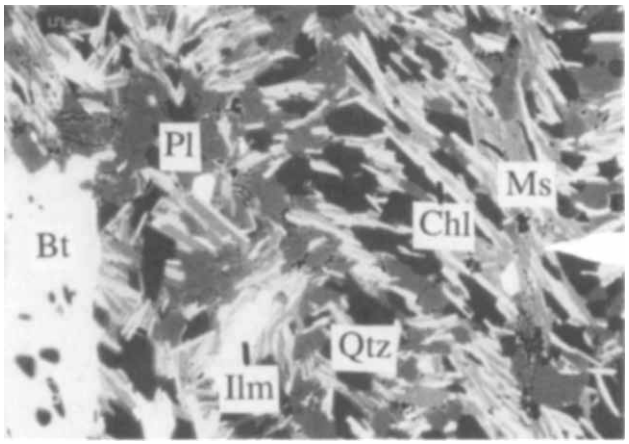

(a)

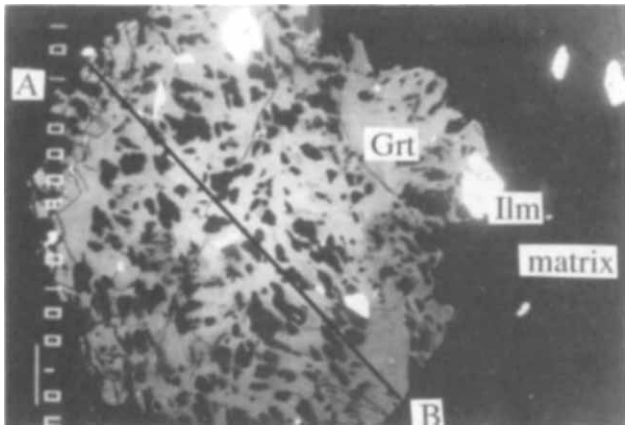

(b)

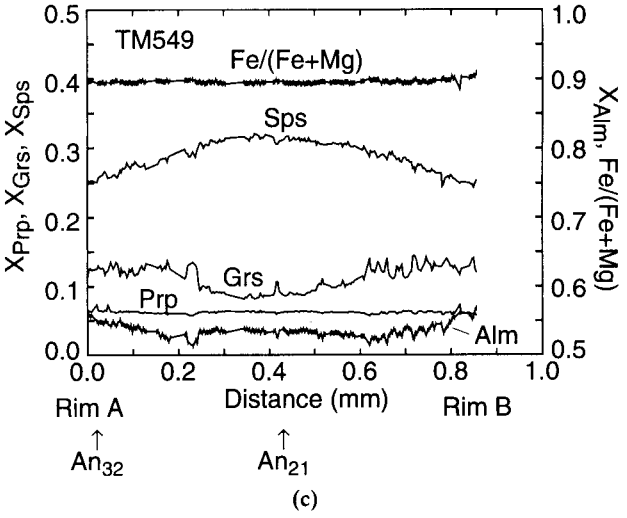

(c)

Fig. 8. Sample TM549 from the M3 garnet isograd west of Union Village. (a) Backscattered electron image showing F2 crenulation of the chlorite + muscovite S1 schistosity. Biotite and plagioclase overgrew the crenulation foliation. Width of view = 560 μm. (b) Backscattered electron image of garnet that overgrew the F2 crenulation. Compositional zoning appears as shades of grey. Quartz inclusions (black) may have been partially consumed during garnet growth. Scale bar = 100 μm. (c) Garnet compositional zoning along traverse in (b). The scale for Fe/(Fe + Mg) and X_{Alm} is shown to the right, and the scale for X_{Prp}, X_{Sps} and X_{Grs} is shown to the left. Tic marks on Fe/(Fe + Mg) and X_{Alm} show positions of analyses. Also shown is the correlation of matrix plagioclase compositions to garnet zoning (arrows) that was used in thermobarometry (Fig. 4).

for Field Trips in Vermont, Vol. 2 (ed. Westerman, D. S.), pp. 109–133. New England Intercollegiate Geological Conference.

White, W. S. & Eric, J. H., 1944. Preliminary report on the geology of the Orange County copper district, Vermont. *United States Geological Survey Open-File Report.*

White, W. S. & Jahns, R. H., 1950. Structure of central and east-central Vermont. *Journal of Geology*, **58**, 179–220.

Woodland, B. G., 1977. Structural analysis of the Silurian-Devonian rocks of the Royalton area, Vermont. *Geological Society of America Bulletin*, **88**, 1111–1123.

Received 7 July 1993; revision accepted 10 May 1994.

APPENDIX: SAMPLE DESCRIPTIONS

East flank of Strafford Dome

Garnet zone; sample TM549

Sample TM549 is a calcic pelite from the M3 garnet isograd 1.8 km north-west of Union Village (Fig. 2). The matrix assemblage is garnet + biotite + chlorite + plagioclase + quartz + muscovite + ilmenite + apatite + tourmaline. The S0 compositional layering is marked by differing proportions of quartz and mica. S1 is a muscovite + chlorite foliation parallel to S0 and was crenulated by S2 (Fig. 8a). The peak metamorphic minerals garnet, microporphyroblastic biotite and plagioclase overgrew the S2 fabric (Fig. 8a,b). Garnet has abundant inclusions of quartz, and fewer inclusions of chlorite, ankerite, apatite and ilmenite. Thus, garnet is inferred to have grown by the reaction

$$\text{Chl} + \text{Ank} + \text{Ms} + \text{Qtz} = \text{Grt} + \text{Bt} + \text{Pl} + \text{fluid}.$$

Garnet is zoned, with decreasing X_{Sps} and increasing X_{Grs} from core to rim (Fig. 8c). Plagioclase is zoned from An_{21-24} in the core to An_{32} on the rim. Plagioclase occurs throughout the rock, and some grains (with An_{21} cores) overgrew the S2 mica foliation. Cores of garnet are correlated with plagioclase cores, as are garnet and plagioclase rims, because both minerals post-date S2.

Garnet–biotite thermometry (Hodges & Spear, 1982) and garnet–biotite–muscovite–plagioclase barometry (Hodges & Crowley, 1985; Powell & Holland, 1988, as modified by Spear *et al.*, 1991, for the garnet activity model of Hodges & Spear, 1982; Hoisch, 1990) give *P–T* ranges centred at 475° C and 4500 bar for both the garnet core and rim using the matrix biotite (Fig. 4). The compositional zoning was produced during a change of *P–T* conditions small enough to be unresolvable by thermobarometry.

Garnet did not grow in this location during M2, in contrast with locations to the west (see below), where garnet grew pre-, syn- and post-D2. Consequently, an M2 garnet isograd can be drawn west of this sample separating locations where M2 was at biotite zone from locations where M2 produced garnet (Fig. 3).

Staurolite zone: samples TM534 and TM445

Samples TM534 and TM445 were described by Menard & Spear (1993). Both samples are calcic pelitic schists from the staurolite zone; TM445 has staurolite that overgrew the S1 and S2 fabrics, whereas TM534 does not have staurolie. The *P–T* paths for garnet growth for both samples (Fig. 4) are dominated by heating that followed the development of the S2 fabric, as shown by microfabrics.

Kyanite zone: sample TM825A

Sample TM825A from the kyanite zone was also described by Menard & Spear (1993). The microfabrics show that the garnet core grew prior to S2, in contrast with sample TM549, and the rim later than S2. A P–T path (Fig. 4) was calculated using garnet zoning and abundant plagioclase inclusions and has an initial increase of temperature during growth of the garnet core, followed by a 1.5 kbar pressure increase during D2 crenulation.

Garnet grew at similar temperatures in samples TM825A and TM549, but the fabrics show that the garnet cores grew at different times with respect to D2 deformation in rocks at different structural levels. Neverthelsss, the garnet rim in sample TM825A may correlate temporally with garnet in sample TM549, since both overgrew D2 fabrics, but the correlation is tenuous. This correlation would suggest several kilometres of differential uplift between the two samples because the garnet rim in sample TM825A grew at 4–6 kbar higher pressure and 10–50° C higher temperature than garnet in sample TM549. Alternatively, if the thermal peak of metamorphism in the two rocks was synchronous, that would also suggest several kilometres of differential uplift. As a third possibility, if the peak recorded pressures were synchronous, that would also require several kilometres of differential uplift. The possibility that there was no differential uplift between these samples cannot be ruled out, but seems unlikely.

Garnet growth was followed by continued growth of matrix plagioclase with increasing X_{An}, indicating heating with a possible decrease of pressure (Menard & Spear, 1993).

Kyanite zone: sample TM590

Sample TM590 is from Morrill Mountain 1 km north-east of the Elizabeth Mine (Fig. 2). Textures in this sample are typical of the highest grade metapelites in the lower part of the Gile Mountain Formation. The matrix assemblage is kyanite + staurolite + garnet + biotite + plagioclase + quartz + muscovite + ilmenite + rutile + zircon + tourmaline + graphite. Garnet has inclusions of epidote, plagioclase, rutile, ilmenite, quartz and zircon. The garnet core is marked by abundant, small inclusions of titanite and ilmenite that define a straight, included S1 fabric, whereas the outer portion of the garnet lacks titanite and has few ilmenite inclusions, which obscures the trend of the inclusion trails in the rim. The matrix S2 fabric is deflected around the garnet core, but the garnet rim overgrew the S2 fabric.

Staurolite cross-cuts the S2 fabric and has inclusions of biotite, chlorite, ilmenite, epidote, allanite, quartz, apatite and An_{34} plagioclase. Kyanite also cross-cuts the S2 fabric, suggesting that the temperature increased after D2.

P–T conditions for the end of garnet growth of approximately 550° C and 8500 bar (Fig. 4) were computed using garnet near-rim compositions, An_{34} plagioclase correlated from staurolite inclusions and the S2 micas. These conditions are similar to those computed for various parts of the P–T path in TM825A, but are significantly higher than pressures and temperatures for sample TM549.

Core of Strafford Dome: sample TM732

Sample TM732 is from the Waits River Formation in the core of the Strafford Dome (Fig. 2). A calcic pelite assemblage of kyanite + garnet + biotite + plagioclase + calcite + epidote + quartz + muscovite + ilmenite + rutile + tourmaline + retrograde chlorite is interlayered at a centimetre scale with an impure marble assemblage of quartz + calcite + biotite, with lesser amounts of rutile + ilmenite + muscovite + tourmaline. The micas are foliated parallel to the compositional layering. No obvious relics of S1 are present, and the dominant matrix fabric is interpreted as S2 on the continuity of style, intensity and orientation of fabrics from the core of the dome to the flanks where S1 and S2 are readily distinguishable (White & Jahns, 1950).

Matrix epidote, calcite, chlorite, sodic plagioclase and some of the muscovite are retrograde minerals. Epidote in calcic pelite layers occurs in fine-grained aggregates intergrown with quartz that cross-cut S2 micas and matrix plagioclases. Chlorite and the most sodic plagioclase, An_{37}, partially replaced S2 biotite.

Garnet has inclusions of quartz, epidote, graphite, plagioclase and ilmenite. Inclusion trails in the garnet have a spiral pattern with an apparent rotation of 270° (Fig. 9a). Garnet has pressure shadows next to it in the dominant S2 foliation (horizontal in Fig. 9a) and the inclusion trails in garnet appear to merge into S2, suggesting that garnet grew during the D2 deformation. Garnet is zoned, with X_{Grs} increasing steadily from the core to near the rim (Fig. 9b). In the outer 15 μm of the garnet, however, X_{Grs} decreases sharply while X_{Sps} and Fe/(Fe + Mg) increase.

The garnet rim was partially replaced by plagioclase zoned from An_{51} to An_{67} and, thus, garnet grew prior to this increase of X_{An}.

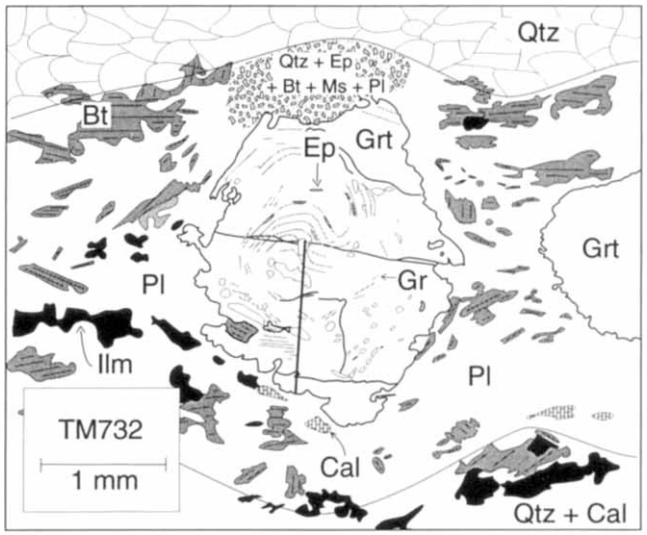

(a)

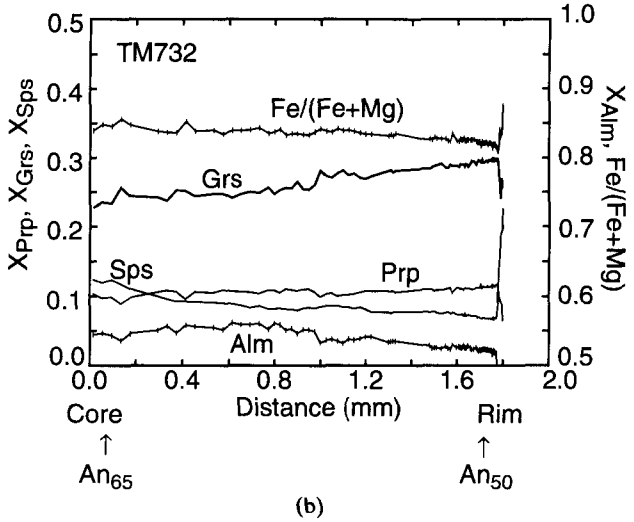

(b)

Fig. 9. Garnet in TM732 from the core of the Strafford Dome. (a) Sketch showing the spiral pattern of inclusion trails in garnet. The dominant matrix foliation, S2, is horizontal in the sketch. (b) Garnet compositional zoning along the traverse shown in (a). The scale for X_{Prp}, X_{Sps} and X_{Grs} is shown to the left, and the scale for Fe/(Fe + Mg) and X_{Alm} is shown to the right. Arrows show correlation of matrix plagioclase compositions to the garnet zoning used in the P–T path (Fig. 5 and Table 1).

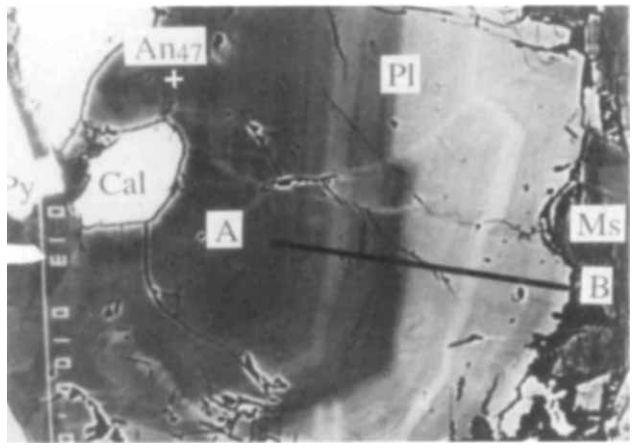

(a)

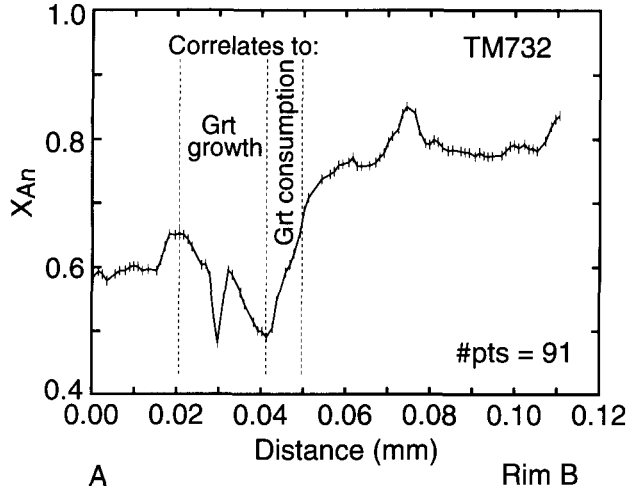

(b)

Fig. 10. Plagioclase in a shadow of garnet in sample TM732. (a) Backscattered electron image showing growth zoning. Pyrite and calcite are part of the retrograde assemblage and post-date the plagioclase. Location of traverse A–B is shown. Width of view = 220 μm. (b) Plagioclase compositions in sample TM732 along the traverse shown in (a). This plagioclase grain is interpreted to record a nearly complete sequence of plagioclase compositions. Core composition (inward of point A on traverse) is An_{47}.

Plagioclase composition at some point during garnet growth was near An_{65}, as shown by six inclusions in the garnet. Interpretation of the change of plagioclase compositions during garnet growth, however, is less direct. The overall sequence of plagioclase compositions is shown in a plagioclase grain in the pressure shadow of a garnet (Fig. 10): X_{An} increased from An_{47} in the core to An_{83} at the rim, with several changes of compositional trend. Figure 10 also shows the interpreted correlation of plagioclase zoning with garnet growth and consumption. Since plagioclase is the only major Na-bearing phase, the inferred decrease of X_{An} during garnet growth suggests that plagioclase was a reactant at the time, which may explain the absence of An_{60-50} plagioclase inclusions in the garnet.

Chlorite was in the assemblage during garnet growth, as shown by comparison with samples at lower grade (e.g. sample TM549). We interpret garnet to have grown at the expense of chlorite and plagioclase by the reaction

$$Chl + Pl + Ep + Ms + Qtz + Gr = Grt + Bt + H_2O + CO_2.$$

After the removal of chlorite from the assemlage, garnet was partially consumed and plagioclase grew with X_{An} increasing to An_{85}, possibly by the reaction

$$Grt + Ep + Ms + Qtz + Gr = Bt + Pl + H_2O + CO_2.$$

Thermometry for sample TM732 (Fig. 5) using the lowest Fe/(Fe + Mg) garnet compositions near the rim of the garnet, An_{50} plagioclase (Fig. 6a) and matrix mica compositions gives pressures of 7–9 kbar with poorly constrained temperatures. The garnet rim with matrix biotite gives maximum recorded temperatures centred near 590° C. The garnet, however, probably grew at temperatures somewhere in the range 500–550° C, based on unpublished data from other rocks (Menard, 1991). Three Gibbs method P–T paths for garnet growth (Fig. 5) computed using three fluid compositions (Table 1) have a nearly isothermal pressure increase of 1.5 kbar, which correlates with D2 deformation using the microfabrics described above.

Subsequent plagioclase growth with increasing X_{An} indicates a P–T trajectory with increasing temperature, decreasing pressure or both (Menard & Spear, 1993). The similarity of pressures between this sample and samples TM825A and TM590 indicates that there was little differential uplift near the centre of the dome.

West flank of Strafford Dome: sample TM458A

Sample TM458A is a calcic pelite from the Waits River Formation at Standing Pond on the west flank of the Strafford Dome (Fig. 2). The matrix assemblage is garnet + biotite + plagioclase + quartz + muscovite + rutile + ilmenite + tourmaline + apatite + zircon. The garnet has inclusions of plagioclase, quartz, ilmenite and epidote. Epidote inclusions occur in the garnet from the centre to near the edge of the garnet. Gently curved S1 inclusion trails in the garnet (Fig. 11a) are continuous with the matrix fabric near the garnet rim, but the S2 fabric drapes over the garnet. Thus, garnet grew during D2, probably in the assemblage garnet + biotite + chlorite + plagioclase + epidote + muscovite + quartz + graphite + ilmenite.

The X_{Grs} zoning defines several regions in the garnet (Fig. 11): the core from the centre of the garnet to the step decrease of X_{Grs} (at 2 mm in Fig. 11b), which coincides with the development of the S2 fabric; the rim in the outer 250 μm with low X_{Grs}; and the edge where Fe/(Fe + Mg) and X_{Sps} increase without a corresponding change of X_{Grs}, reflecting minor diffusional re-equilibration during cooling (Spear *et al.*, 1991).

Plagioclase inclusions in the garnet interior have compositions in the range An_{21-43}. Individual plagioclase inclusions are zoned, with increasing X_{An} from core to rim. The rim compositions of these plagioclase inclusions change from An_{25} in the centre of the garnet to An_{43} in the outer core (Fig. 11b). Plagioclase that replaced garnet is zoned from An_{34} to An_{39}, suggesting an increase of X_{An} after garnet growth ended. Matrix plagioclase that overgrew the S2 foliation has similar compositions (zoned from An_{18} to An_{32}) as inclusions in the garnet.

Thermobarometry using garnet compositions near the rim with the lowest Fe/(Fe + Mg) (Fig. 5), An_{32} plagioclase correlated from the matrix and the matrix S2 micas gives P–T conditions of 530–570° C and 8–9 kbar. A Gibbs method P–T path (Fig. 5, Table 2) computed for garnet growth indicates heating during growth of the garnet core, followed by a 1 kbar increase of pressure during D2 deformation, with continued heating during growth of the garnet rim.

Townshend–Brownington Syncline

Sample TM747

Sample TM747 is a pelite from the White River in North Royalton in the core of the Townshend–Brownington Syncline (Fig. 2). S0 is graded bedding with a gradational change from quartz + muscovite-rich layers to muscovite + graphite-rich layers. The

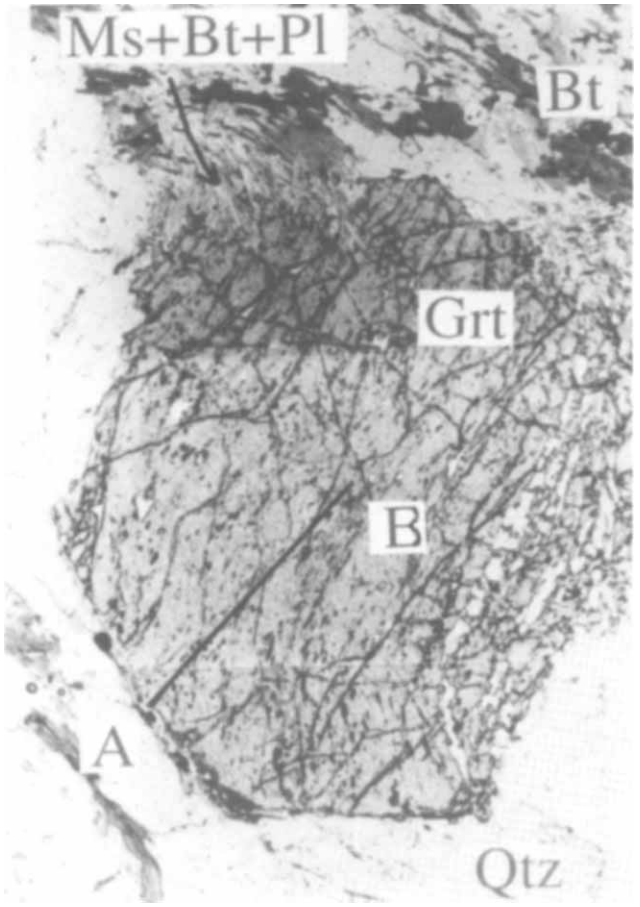

(a)

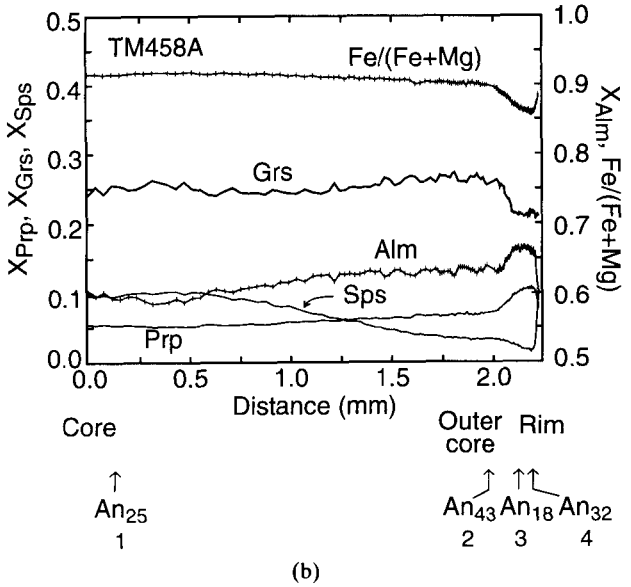

(b)

Fig. 11. Garnet in sample TM458A from Standing Pond on the west flank of the Strafford Dome. (a) Photomicrograph of garnet. Inclusion trails inside the garnet and well-developed pressure shadows (not clearly visible) around the garnet show that the garnet grew during the formation of the S2 fabric. Inclusion trails curve into the matrix S2 orientation within 0.2 mm of the rim (not clearly visible). The top edge of the garnet was replaced by an intergrowth of muscovite + biotite + plagioclase. Length of traverse A–B is 2.5 mm. Plane polarized light. (b) Garnet compositional zoning along traverse A–B. The scale for X_{Prp}, X_{Sps} and X_{Grs} is shown to the left, and the scale for Fe/(Fe + Mg) and X_{Alm} is shown to the right. The increase of Fe/(Fe + Mg) at the rim reflects diffusional re-equilibration during cooling. Arrows show correlations between plagioclase and garnet compositions used in the P–T path (Fig. 5 and Table 2). Plagioclase compositions are from inclusions in the garnet (at points 1 and 2) and from matrix plagioclase (at 3 and 4).

matrix assemblage is garnet + biotite + plagioclase + quartz + muscovite + graphite + tourmaline + chlorite + ilmenite. In addition, quartz-rich layers contain epidote near the boundaries with muscovite + graphite-rich layers, and contain minor staurolite. Ilmenite is aligned in S1, was rotated by F2 folding and has pressure shadows in the S2 fabric (Fig. 12a). Retrograde chlorite porphyroblasts cross-cut the S2 fabric, and partially replaced garnet (Fig. 12b) and staurolite.

Garnet has inclusions of quartz, plagioclase, epidote, zircon, ilmenite and graphite. The ilmenite inclusions, in turn, have inclusions of muscovite, biotite, chlorite and plagioclase. Garnets in quartz-rich layers (Fig. 12b) have graphite inclusions that define gently folded S1 inclusion trails, indicating that initial garnet growth post-dates S1. The matrix S2 foliation drapes around the garnet, showing that garnet was present during D2. Garnet compositional zoning (Fig. 12c) is similar to that in sample TM458A (Fig. 11b).

Plagioclase inclusions in the core of the garnet are zoned, with increasing X_{An} from core to rim. Rim compositions of these plagioclase varies from An_{19} in the centre of the garnet to An_{32} in the outer core (Fig. 12c). Plagioclase inclusions within ilmenite inclusions in the rim of the garnet have compositions of An_{21-23}. Plagioclase in S2 pressure shadows is zoned from An_{21} to An_{16} from core to rim; these grains appear to have been protected from D2 deformation and preserve the oldest matrix plagioclase. The youngest matrix plagioclase overgrew the S2 fabric and is zoned from An_{17} to An_{26} from core to rim. Inclusions of An_{19} plagioclase in staurolite, which overgrew the S2 fabric, may correlate with this final increase of X_{An}.

Thermobarometry for sample TM747 for the garnet near-rim, An_{21} plagioclase inclusions in ilmenite inclusions in garnet, and the matrix S2 micas gives P–T estimates centred at 550° C and 9800 bar (Fig. 6). A Gibbs method P–T path (Fig. 6) for garnet growth in sample TM747 (Table 2) indicates heating during growth of the garnet core, followed by a pressure increase of 2 kbar during D2. Temperature continued to increase after the garnet stopped growing, as indicated by M3 staurolite growth. This rock does not record the pressure decrease during late heating seen in samples TM732 and TM825A in the Strafford Dome.

Sample TM914D

Sample TM914D is from Gee Hill in the core of the Townshend–Brownington Syncline (Fig. 2). This rock is similar to sample TM747, but contains trace amounts of paragonite in S1 orientations. The garnet core has straight inclusion trails of quartz and ilmenite, which curve into the matrix S2 fabric near the garnet rim (Fig. 13a). X_{Grs} is constant across the garnet core, and decreases near the rim (Fig. 13b). The change of X_{Grs} trend occurred later than development of the S2 crenulation, as shown by inclusion trails in the garnet (Fig. 13), and does not reflect a tectonic event and a change of P–T trajectory. Rather, the zoning pattern suggests that a Ca-bearing phase, such as epidote, was present during growth of the garnet core and was removed prior to growth of the garnet rim (Menard & Spear, 1993). Garnet was partially replaced by chlorite during retrograde metamorphism.

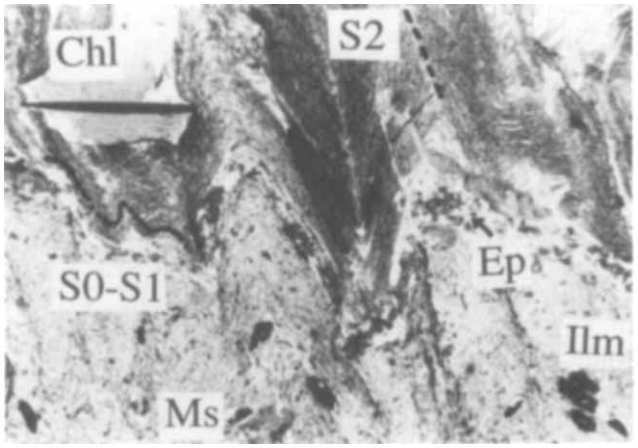

(a)

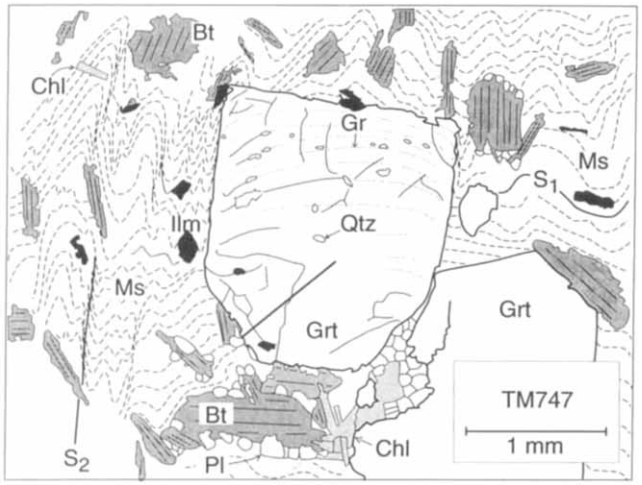

(b)

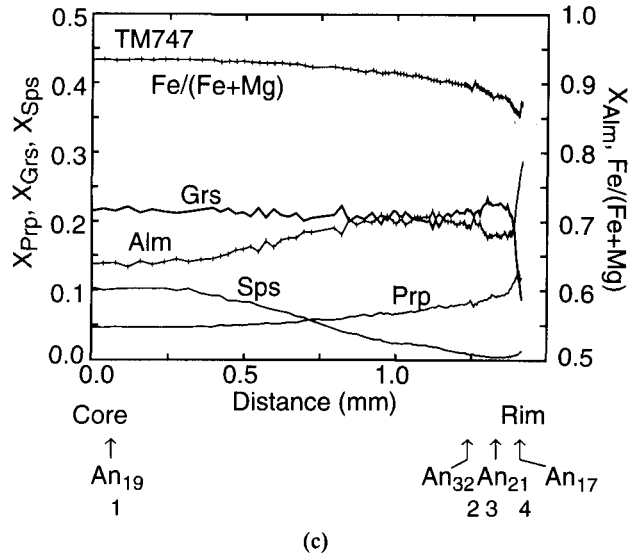

(c)

Fig. 12. Sample TM747 from the Townshend–Brownington Syncline. (a) Photomicrograph of compositional layering S0, foliation S1 and crenulation S2. Ilmenite needles in more graphitic, darker layers have pressure shadows filled with biotite and chlorite. Epidote occurs only in the quartz-rich layers near the compositional break. Width of view = 5.4 mm, plane polarized light. (b) Sketch of a thin section in plane polarized light showing faint trails of graphite (Gr) inclusions that describe a gently curved S1 foliation in the garnet core. The trails curve more sharply near the garnet rim. Matrix biotite and chlorite overgrew the S2 fabric. (c) Garnet compositional zoning along the traverse shown in (b). The scale for X_{Prp}, X_{Sps} and X_{Grs} is shown to the left, and the scale for Fe/(Fe + Mg) and X_{Alm} is shown to the right. Arrows show correlations of plagioclase and garnet compositions used in the P–T path (Fig. 6 and Table 2). Plagioclase compositions are from garnet inclusions (at points 1 and 2) and from the matrix (at 3 and 4).

Biotite also occurs as porphyroblasts with inclusions of quartz and plagioclase. Some biotite porphyroblasts have straight S1 inclusion trails of graphite (Fig. 13c) and pressure shadows in the S2 fabric, but are undeformed. In contrast, biotite in other rocks from the study area was crenulated during deformation. Some biotite porphyroblasts have square corners and roughly rectangular to trapezohedral shapes; other grains are rounded against the S2 foliation. These features suggest that biotite pseudomorphed a porphyroblast that overgrew the S1 muscovite + biotite foliation and was present during the D2 deformation. Thus, the pseudomorphed porphyroblast grew at temperatures between the first appearance of biotite and of garnet. The identity of the pseudomorphed mineral is unknown.

Maximum recorded metamorphic P–T conditions for this sample were near 550° C and 8.5 kbar (Fig. 6). These pressures are 0.5–1 kbar lower than those computed above for sample TM747.

West of the RMC: sample TM742

Sample TM742 is a calcic pelite from the Ordovician Missisquoi Formation at Bethel west of the RMC (Fig. 2). Deformational fabrics and metamorphic grade are continuous across the RMC. The matrix assemblage is garnet + biotite + plagioclase + quartz + muscovite + ilmenite + graphite. Garnet has inclusions of ilmenite, plagioclase, epidote, quartz and tourmaline. The garnet core has sigmoid-shaped inclusion trails with a 120° rotation (Fig. 14a) that end at a textural discontinuity with abundant graphite and ilmenite aligned parallel to the face of the garnet. Inclusions in the garnet rim have orientations similar to the matrix. These features show that the garnet core grew during the development of the D2 crenulation, and that the rim grew later.

Figure 14(b) shows garnet zoning. X_{Grs} is flat in the core, increases by 0.03 at the core–rim boundary marked by the change in inclusion trail patterns, and decreases towards the edge of the garnet. Rim compositions of seven plagioclase grains included near the garnet rim increase from An_2 to An_{20} towards the garnet edge. These inclusions are themselves zoned, with increasing X_{An} towards their rims. The same trend is seen in the matrix, where plagioclase that overgrew the S2 fabric is zoned from An_2 in the core discontinuously to An_{19} and continuously to An_{24} at the rim.

Thermobarometry in sample TM742 (Fig. 6) for the garnet rim with An_{20} plagioclase inclusions and matrix micas gives P–T estimates centred at 540° C and 8000 bar. These post-D2 conditions are similar to those computed for samples from the Northfield Formation nearby at Bethel (unpubl. data), as well as samples from the Townshend–Brownington Syncline (TM914D, TM747). Moreover, the decrease in Fe/(Fe + Mg) towards the rim of garnet suggests an increase in temperature during late garnet growth (Menard & Spear, 1993). A P–T path is not computed for this sample because of the lack of plagioclase inclusions in the garnet core, and because the low-X_{An} plagioclase compositions included in the garnet are inappropriate. The similarity of microfabrics across the RMC also suggests that the development of S2 in this sample also involved a pressure increase in these rocks, as it did in samples discussed above.

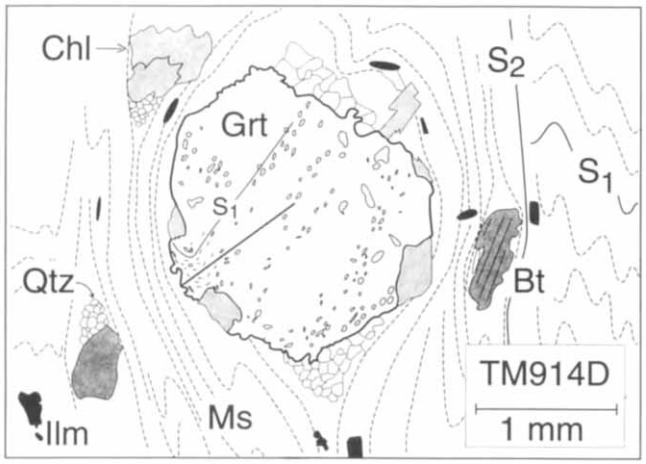

(a)

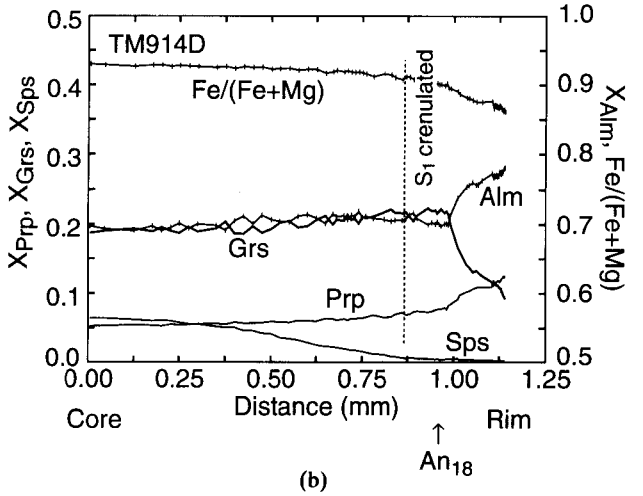

(b)

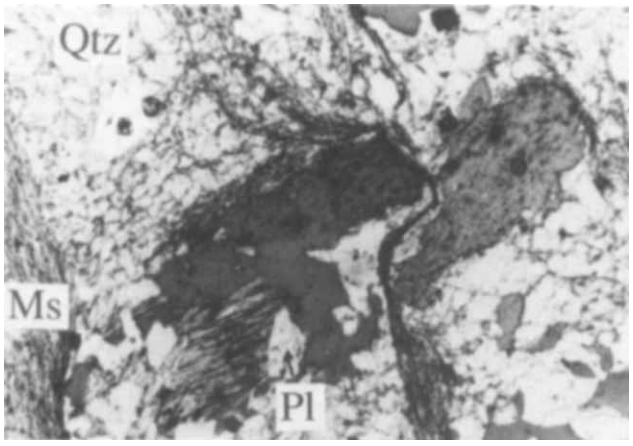

(c)

Fig. 13. TM914D from the Townshend–Brownington Syncline. (a) Sketch of a thin section in plane polarized light. The garnet core overgrew a nearly straight S1 fabric and the rim overgrew the S2 fabric, as shown by the inclusion trails. The garnet rim was partially resorbed and replaced by chlorite. (b) Garnet compositional zoning along the traverse shown in (a). The scale for X_{Prp}, S_{Sps} and X_{Grs} is shown to the left, and the scale for Fe/(Fe + Mg) and X_{Alm} is shown to the right. The change of trend of X_{Grs} occurs well beyond the first inclusions with S2 orientations and reflects the loss of a calcic phase such as epidote from the assemblage. Arrow points to the garnet composition used in thermobarometry (Fig. 6). (c) Photomicrograph of biotite pseudomorphs. The porphyroblasts have roughly rectangular outlines partly modified by consumption during D2. Width of view = 5.4 mm, plane polarized light.

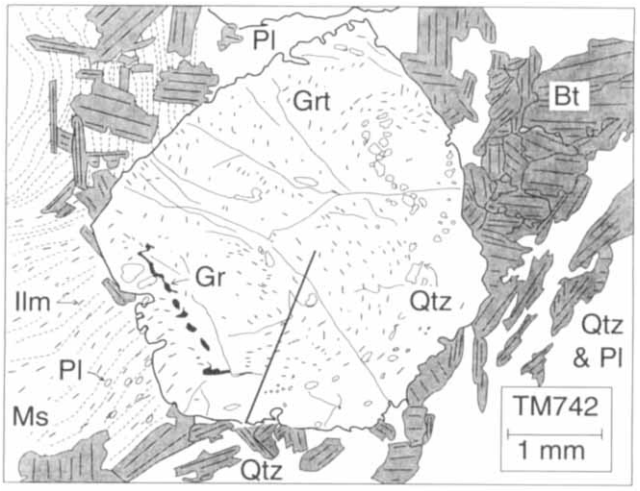

(a)

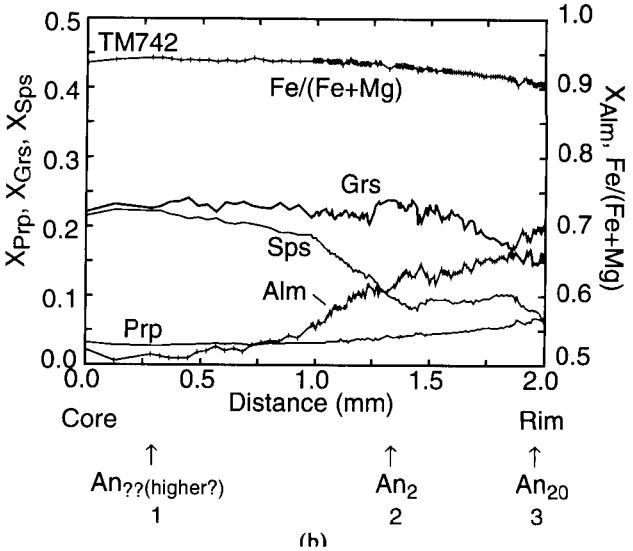

(b)

Fig. 14. Sample TM742 from Bethel on the west side of the RMC. (a) Sketch of a thin section in plane polarized light. The garnet core has a spiral inclusion trail, and the rim has the same pattern of crenulated inclusion trails as seen in the matrix. (b) Garnet compositional zoning along traverse shown in (a). The scale for X_{Prp}, X_{Sps} and X_{Grs} is shown to the left, and the scale for Fe/(Fe + Mg) and X_{Alm} is shown to the right. Correlated plagioclase compositions are from inclusions in garnet.